Reprinted from: *Mesoscale/Synoptic Coherent Structures in Geophysical Turbulence*, edited by J.C.J. Nihoul and B.M. Jamart

NUMERICAL MODELING OF AGULHAS RETROFLECTION AND RING FORMATION WITH ISOPYCNAL OUTCROPPING

D. B. BOUDRA, K. A. MAILLET, AND E.P. CHASSIGNET[1]
Rosenstiel School of Marine and Atmospheric Science, University of Miami,
4600 Rickenbacker Causeway, Miami FL 33149-1098, (USA)

ABSTRACT

Experiments with a pure-isopycnic coordinate numerical model on a domain representing the oceanic region within a few thousand kilometers of South Africa and in which isopycnal outcropping is allowed around the edges of the Agulhas Current Retroflection and Agulhas rings are described. Previous experiments with a quasi-isopycnic coordinate model have exhibited a vigorous retroflection and active ring formation for certain parameter ranges. But mean layer thickness choices have been such that isopycnal outcropping was confined to the model subpolar gyre interior to the southwest of the retroflection. In order to make more close comparison with observation and with analytical theory describing the behavior of warm lenses, we invoke the unique aspect of the pure-isopycnic coordinate model which allows coordinate surfaces to outcrop as do density surfaces in frontal zones. Four new experiments are described, proceeding from a 3-layer case—in which the first interface density jump is decreased by 50% compared to previous experiments—to a 5-layer case with three layers in the mean upper 250 m. Isopycnal outcropping along the subtropical convergence and around the edge of the Indian Ocean subtropical gyre is a primary feature of three of the new experiments. In addition, some characteristics of ring formation are more realistic than in previously published experiments: e.g., it is more frequent and is typically west or southwest of the Agulhas Bank tip as opposed to on the southeast side. The new experiments are generally less energetic. Energy input by the wind is pumped into the lower layers and dissipated more efficiently. For very thin upper layers, an inequity develops between the mean upper layer thicknesses in the Indian and Atlantic Oceans: the top layer fluid tends to become trapped in the Atlantic Ocean. This, in turn, has an impact on the dynamics of the retroflection and ring formation. These must, therefore, be viewed as preliminary outcropping experiments. It is concluded that, in the future, some account must be made for thermodynamic forcing, by which upper layer Atlantic Ocean water downwells and returns along intermediate isopycnals to the Indian Ocean where it then upwells back into the top layer.

INTRODUCTION

The Agulhas Current Retroflection region off the tip of South Africa is the birthplace of some of the largest and most powerful warm core rings in the world ocean (see, e.g., Olson and Evans, 1986; Lutjeharms and Gordon, 1987). These eddies separate from the western edge of the Retroflection several times a year (Lutjeharms, 1981) and drift into the subtropical South Atlantic. There can be no doubt that they play an important role in the transfer of warm, salty thermocline water from the Indian into the South Atlantic Ocean (Gordon, 1985). In addition, it has been argued that such transfer is a critical link in the world ocean circulation route supplying the North Atlantic with water which eventually

[1]Present address: NCAR, P.O. Box 3000, Boulder CO 80307

undergoes deep convection in the Norwegian/Greenland Sea, in turn, feeding the Atlantic Ocean deep western boundary current (Gordon, 1986). Moreover, the South Indian Ocean subtropical wind gyre supports an annual mean 40 to $50\times10^6\ m^3\ s^{-1}$ transport reaching Africa's tip in the Agulhas Current (Hellerman and Rosenstein, 1983). The proportion of this transport which flows into the Atlantic, either within rings or in leakage around or over the Agulhas Bank, and how much continues northward across the equator can have strong implications for the structure of the South Atlantic subtropical gyre. Thus, as well as being comparatively large and powerful, Agulhas rings exert perhaps the most far-reaching influences among world ocean rings in terms of large scale dynamics and water mass characteristics.

In the early 1980s, we undertook to develop a hierarchy of models of increasing complexity, in which the focal point is the Agulhas Current Retroflection. The principal questions we have sought to answer are *Why does the Agulhas retroflect?*, *What are the dynamics of the variability in the region?*, and *What are the implications of a strong/weak retroflection on the two ocean wind-driven circulation?* In a one-layer, idealized South Atlantic/Indian Ocean numerical model, De Ruijter and Boudra (1985) first showed that a strong retroflection may be established by increasing the Rossby number[2] of the model Agulhas as it separates from the tip of Africa, where with relatively low Rossby number there is little or no retroflection. Furthermore, they determined that it was the corresponding increase in the β-induced gain of relative vorticity which turns the current back toward the Indian Ocean after separation, that is, rather than the increased southward inertia, which had been suggested by De Ruijter (1982). In those barotropic model experiments, Agulhas rings were unrealistically large and energetic. In two- and three-layer experiments on the same model domain, Boudra and de Ruijter (1986), referred to hereafter as BD, varied many of the model parameters which might affect the retroflection strength, and established that the change in the vorticity balance at separation is the primary physical mechanism of retroflection. In these experiments where Africa was represented by a thin rectangle extending a little more than half way into the subtropical wind gyre from the northern boundary of the basin, ring formation and leakage into the Atlantic Ocean was essentially shut off in the most realistic Rossby number cases with 40 km resolution. A corresponding 20 km resolution experiment exhibited four realistic size rings during the ten years of simulation.

Boudra and Chassignet (1988), referred to hereafter as BC, analyzed the vorticity balance of the retroflection region for many of the above experiments and determined that vertical stretching is at least as important as planetary vorticity advection in inducing the positive relative vorticity which turns the Agulhas back toward the Indian Ocean. As the upper ocean Rossby number and baroclinicity was increased,[3] stretching eventually dominated βv in the balance, due mainly to increasing upper layer potential vorticity contrast between the southwest Indian Ocean and the southeast Atlantic. Introducing a new experi-

[2]Obtained by decreasing the model layer thickness.

[3]Obtained by increasing the number of layers and decreasing the top layer thickness.

ment in which the tip of Africa is represented more realistically with the approximate shape of the Agulhas Bank, they obtained more leakage and ring formation. Rings were formed at the rate of approximately three per year in this experiment, termed E11. Neither planetary vorticity advection nor the above-mentioned potential vorticity contrast were as large, so that the retroflection was correspondingly weaker. Ring formation using 20 km resolution was found to be associated with strong barotropic and baroclinic energy conversion in the rectangular Africa case and somewhat weaker mixed conversion in E11 (Chassignet and Boudra, 1988, referred to hereafter as CB). It was concluded that the degree of dynamical instability required for model ring formation depends significantly on the approximation for the shape of the Agulhas Bank shelf break.

In this paper we take a further step in developing a realistic South Atlantic/Indian Ocean model and, at the same time, examine the sensitivity of the model retroflection and ring formation to upper ocean stratification and isopycnal outcropping. In some of the previous 3-layer experiments, substantial variation in isopycnal interface depth was allowed. In the high Rossby number experiments, the uppermost interface was typically 300-350 m shallower on the retroflection edge than in its center. However, the mean upper layer thickness was great enough that isopycnal outcropping occurred only in the southwestern interior of the subpolar gyre and only in the rectangular Africa cases. As is the case along most separated western boundary currents of the world ocean, isopycnal outcropping around the edge of the Agulhas retroflection and Agulhas rings is pronounced (see, e.g., Gordon, 1985). In fact, several theoretical models of boundary current separation require the pycnocline/thermocline to surface (e.g., Charney, 1955; Parsons, 1969; Veronis, 1973; Moore and Niiler, 1974; Ou and de Ruijter, 1986) at which point the current, which is isolated above the thermocline, must separate. Isopycnal layered numerical models which solve the primitive equations as initial/boundary value problems over a 3-dimensional grid volume have traditionally been hampered from allowing such interface surfacing because of numerical difficulties encountered when layer thickness is allowed to shrink to zero. One way in which the difficulties have recently been overcome was developed and tested by Bleck and Boudra (1986): that is, the Flux-Corrected Transport (FCT) algorithm, originally developed by Boris and Book (1973) and extended to multi-dimensional applicability by Zalesak (1979), is used to solve the continuity (layer thickness tendency) equation. Within this framework, coordinate layers are allowed to collapse at the upper or lower boundary (and even in the interior) in a numerically trouble-free fashion.

In this investigation of model retroflection sensitivity to upper ocean stratification, we therefore incorporate the FCT pure-isopycnic coordinate model[4], replacing Bleck and Boudra's (1981) hybrid (quasi-isopycnic) coordinate model[5] used in the previous multi-layer experiments. The new model and numerical differences from the quasi-isopycnic model are briefly described in Section 2, where the experimental setting and a table of experiments

[4]Referred to hereafter as the pure-isopycnic model.
[5]Hereafter referred to as the quasi-isopycnic model.

to be discussed are also given. In Section 3, the experimental results are characterized in a general sense, setting the stage for a discussion of ring formation and behavior among the experiments in Section 4. In the final section, we summarize results of this sensitivity study and point to additional experimentation which will help determine the validity of the preliminary conclusions and yield new insight into the dynamics of Agulhas retroflection and ring formation.

2 THE MODELS AND THE EXPERIMENTAL SETTING

2.1 The Models Used

The primitive equation, pure-isopycnic model may be viewed as a stack of shallow water models, each consisting of a momentum and a continuity equation:

$$\frac{\partial \vec{v}}{\partial t} + \frac{1}{2}\nabla_\rho \vec{v}^2 + \eta \hat{k} \times \vec{v} = -\nabla_\rho M + \alpha \frac{\partial \vec{\tau}}{\partial z} + A(\delta_\rho p)^{-1} \nabla_\rho \cdot \delta_\rho p \nabla_\rho \vec{v} - \sigma \vec{v}, \tag{1}$$

$$\frac{\partial}{\partial t}(\delta_\rho p) + \nabla_\rho \cdot (\vec{v} \delta_\rho p) = 0, \tag{2}$$

where $\eta = \xi + f$ is the absolute vorticity ($\xi = v_x - u_y$); $M = gz + p\alpha$ is the Montgomery potential; the "layer pressure-thickness" $\delta_\rho p$ is the thickness of a layer of constant density; the specific volume $\alpha = \rho^{-1}$; τ is the wind stress; A is the lateral viscosity; and the bottom drag coefficient σ is zero except in the bottom layer. The subscript ρ indicates derivatives on surfaces of constant density. These shallow water models communicate vertically through hydrostatically transmitted pressure forces, according to

$$\frac{\partial M}{\partial \alpha} = p. \tag{3}$$

The quasi-isopycnic model consists, in addition, of a thermodynamic equation, which is of consequence in regions of a layer where density varies. The horizontal pressure force is expressed in terms of both geopotential and pressure gradients along coordinate interfaces, and the momentum and continuity equations also include vertical advection terms. The horizontal derivatives are with respect to the generalized coordinate s rather than density *per se*. For details on how the vertical motion $\dot{s}$ is computed, the reader is referred to Bleck and Boudra (1981). In the experiment E11, no deterioration of the isopycnal character of the layers was encountered, so that the model behaved as a pure-isopycnic one.

In two primary ways, the numerical integration of the pure- and quasi-isopycnic models differs. First, in the quasi-isopycnic model, the continuity equation is formulated in 2nd-order centered finite difference form and integrated forward with leap frog. In the pure-isopycnic model, mass fluxes into and out of grid boxes are initially estimated using 1st-order, upstream approximations. Those fluxes are then corrected by means of *anti-diffusive* fluxes determined by the difference between the first order and some higher order[6] approximation—that is, assuming full incorporation of the anti-diffusive fluxes would yield non-negative layer thickness. If the latter condition is not satisfied, the low and high order

[6] In the present case, 2nd order.

approximations are blended, so that negative thickness is avoided. For more detail, see Bleck and Boudra (1986).

The second difference in the model numerical integrations is related to the allowance of zero layer thickness in the pure-isopycnic model. Bleck and Boudra (1981) formulated the finite differences of the third term on the left of (1) such that the nonlinear terms in the quasi-isopycnic model conserve potential vorticity and potential enstrophy, provided the coordinate surfaces remain isentropic (isopycnic). In the strict sense, this is not possible in the pure-isopycnic model because of a division by layer thickness, which may vanish. It is likely that some provision can be made for a conservative formulation in regions where layer thickness is bounded away from zero and a smooth transition to a nonconservative operator in outcropping zones. Such has not been attempted in the experiments to be described here, however, and instead a less conservative formulation has been used. On the other hand, the outcome of the two formulations must converge as grid spacing tends to zero—that is, as the numerical solutions tend to the exact solution. Boudra and Chassignet (1988) found that the conservation terms in the quasi-isopycnic model spelled the difference between a strong (with conservation) and a weaker (without conservation) retroflection when using 40 km grid spacing. In the specific case of the 20 km horizontal resolution experiment E11, the ten-year integration has since been extended three years, first with the conservative and then with the less conservative formulation. The mean flow patterns and the mean and eddy energy fields of these two extensions have very small differences. It is felt, therefore, that the use of 20 km resolution here is sufficient to avoid large errors which might result from lack of exact potential vorticity and potential enstrophy conservation.

The models are configured on the basin depicted in Figure 1. The dimensions are many times smaller than those of the South Atlantic/Indian Ocean, but provide an economically convenient domain size for the study of retroflection dynamics. Nevertheless, the eastern and western boundaries, representing Australia and South America, as well as the coast of South Africa, are assigned the no-slip condition, and the northern and southern boundaries free-slip. The steady wind stress profile is shown on the left. The resulting flow pattern yields counterclockwise subtropical gyres east and west of South Africa, an elongated subpolar gyre near the southern boundary, and a region southward from Africa's tip to the latitude of wind curl zero where exchange may occur between the two subtropical gyres, depending on the strength of the model Agulhas retroflection. The northern branch of the subpolar gyre provides an eastward drift along a frontal-type feature with which the model Agulhas may interact, much as the real Agulhas Current system interacts with the northern edge of the Antarctic Circumpolar Current (ACC).

2.2 Experimental Setting and Parameters

The distinguishing parameters and some equilibrium characteristics of the experiments to be discussed here are given in Table 1. The lateral viscosity is $A = 330\ m^2\ s^{-1}$ and bottom drag coefficient $\sigma = 1 \times 10^{-7}\ s^{-1}$ for all the experiments. In the case of E11, the

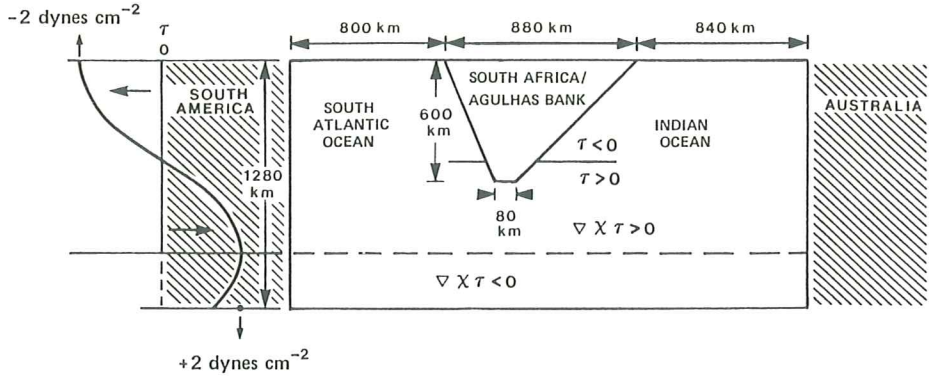

Figure 1: Illustration of the flat bottom model domain and steady zonal wind forcing pattern.

wind stress τ is specified to decrease from its maximum value at the surface to zero at 100 m depth, so that the tendency for interface outcropping is reduced when the layer interface rises above 100 m. In the remaining experiments, the impact of interface outcropping on the solution is of interest. Therefore, the depth over which the wind stress acts directly is reduced to 10 m.

Exp.	Number of layers	Thickness of the layers (db)	g' ($m\ s^{-2}$)	R_d (km)	Mean Total A.P.E. $10^4\ J\ m^{-2}$	Mean Total K.E. $10^4\ J\ m^{-2}$	Mean Retroflection Character
E11	3	300 900 3800	0.02 0.005	29 18	13.0	1.95	Quite strong in layer one. Slightly weaker in layer two.
FCT1	3	300 900 3800	0.01 0.015	40 16	10.2	1.6	Moderately strong in layers one and two.
FCT2	4	150 150 900 3800	0.006 0.004 0.015	40 12 6	10.9	0.9	Rather weak in layers one and two. Stronger in layer three.
FCT3	4	75 175 950 3800	0.003 0.005 0.017	42 11 4	8.9	0.95	None in layer one. Weak in layer two. Modertately strong in layer 3.
FCT4	5	75 75 100 950 3800	0.003 0.003 0.003 0.016	40 10 4 2	9.05	0.82	None in layer one. Very weak in layers 2 and 3. Moderately strong in layer 4.

For all experiments, $\Delta x = 20 km$.

Table 1: Distinguishing parameters and some equilibrium characteristics of the experiments. The basin A.P.E. is area-averaged as is the K.E.

In the fifth column of the Table are the baroclinic radii of deformation R_d corresponding to the basic stratification for each experiment. These only give a rough indication of what the R_d are at any point within the domain after the experiments reach equilibrium. It may be noted, however, especially for experiments FCT2, FCT3, and FCT4, that resolution of the first mode is improved over that of E11, but the higher modes are very poorly resolved by the grid spacing. This results primarily from the decision to decrease the upper ocean g''s and strengthen the g' across the lowest interface in order to encourage interface outcropping as a first-order priority. Adequate resolution of the higher modes would in any case be difficult with 20 km grid spacing. Five and ten kilometer resolution experiments are not currently economically feasible. At the same time, we recognize that increasing the number of vertical modes without also increasing horizontal resolution is open to question. Thus, the results presented here should be viewed mainly qualitatively and in terms of our highest priority. Study of the sensitivity of the model to better high vertical mode resolution must be left for future work.

3 GENERAL REMARKS

The experiments have been examined and intercompared in terms of a number of diagnostic quantities and fields:

1. Time series of basin-averaged kinetic energy in each layer and vertically integrated and of basin available potential energy associated with the layer interfaces and the vertical sum.

2. Vertically integrated and individual layer time-averaged mass transport streamfunctions.

3. Time-averaged layer thickness fields.

4. Horizontal fields of time-averaged total and eddy kinetic energy in each layer and the vertical integral.

5. Horizontal fields of time-averaged R.M.S. interface depths.

6. Time-averaged fields of layer potential vorticity.

7. Series of instantaneous upper ocean mass and flow fields in the center of the model domain.

The following section discusses these experiments in terms of the primary interest in this volume: the coherent structures, Agulhas Rings; that is, how and where the rings form and their subsequent behavior. To set the stage for this discussion, it is first appropriate to make some general comments concerning the equilibrium characteristics of the experiments.

From the right portion of Table 1, we note that the equilibrium energy levels decrease first as the upper ocean static stability is reduced and then as more coordinate layers are

added in the upper 300 db with very little difference between the last two experiments. An energy decrease as upper ocean resolution is increased is in contrast to the result obtained by BD and analyzed by BC and CB, where the number of layers was first increased from 2 to 3 and then the mean thickness of the top layer was reduced from 600 db to 300 db for rectangular Africa experiments. In each case, the mean total potential and kinetic energies increased. Also, however, the largest layer interface g' remained associated with the uppermost layer interface, 0.02 $m\ s^{-2}$ as opposed to a lower interface g' of 0.005 $m\ s^{-2}$ in the 3-layer cases. Here, this distribution is first changed to upper and lower g''s of 0.01 and 0.015 $m\ s^{-2}$, respectively, and then as more layers are introduced near the top, correspondingly weaker g''s are attached to the interfaces, so that the equivalent upper ocean g' is still $\sim 0.01m\ s^{-2}$. The associated energy trends, then, suggest that as static stability is reduced and vertical resolution increased, more efficient means are developed for dissipating the energy input by the wind.

Further, relating columns 4 and 8 in the Table, we find that the strongest retroflection is generally located within the layer which has the largest g' at its base. For E11 this is layer one, but for FCT2, FCT3, and FCT4 it is the layer second from the bottom. In their vorticity balance analysis, BC showed that the model retroflection strength is associated with the magnitude of the planetary vorticity advection and stretching terms as the current separates. Large values of these terms are favored by a coherent, strong Agulhas reaching Africa's tip. In the first case, it is the southward component of motion which induces positive curvature, and in the second, it is the mean potential vorticity contrast between the southwest Indian and southeast South Atlantic Oceans which exerts a torque on fluid attempting to escape westward. In the above experiments, it seems that maintenance of such a coherent current is favored by strong static stability. If the latter is weak between two layers, flows in the upper layer become unstable more rapidly and transfer their energy through fluctuation pressure stresses to the lower layer. It is thus the layer which has the largest g' immediately below it, which tends to exhibit the most coherent mean flow structures, since it receives energy from above but does not as easily transfer it to the next lower layer.

The primary drop in available potential energy in the Table is from E11 to FCT1, where only the static stability is changed. In FCT1, layer 1 kinetic energy is more rapidly lost to layer 2, reducing the vertical shear, and thus the isopycnal tilt between the layers. Layer 2 energy is less rapidly transferred to layer 3, but these are much thicker than layer 1, so that the velocities, and thus the vertical shear, are relatively small anyway. Available potential energy, which is associated with large isopycnal tilt, related through the geostrophic thermal wind to the vertical shear, is thus substantially reduced in FCT1, as well as the other experiments, relative to E11. CB point out that the portion of the kinetic energy associated with the vertical shear flow is directly related to the total available potential energy, and we see a corresponding reduction from the E11 total K.E. in the FCT experiments.

The above conclusions are further confirmed with examination of the individual layer stream function plots, the basin-averaged and horizontal distributions of layer mean and eddy kinetic energy, the layer interface potential energies, and the R.M.S. interface depth deviations. Space is not available here to illustrate the experimental differences in those quantities and fields, but we may briefly summarize them. The intermediate layers are consistently more energetic and the bottom layer less energetic in FCT1-4 than layers 2 and 3, respectively, in E11, particularly in the most dynamically active regions off South Africa and near the confluence of the northward and southward currents at the western boundary (representing the Malvinas/Falkland and Brazil Currents, respectively). In addition, because the layer 1 retroflection is considerably stronger in E11, the recirculation gyre along the coast and east of Africa is much stronger. Associated with this recirculation is more variability and pumping of energy into the lower layers than is found in the other experiments. This is especially evident in the bottom layer mean flow patterns, which reveal where the driving of a mean circulation by the eddies is most clearly distinguished. In FCT1-4 the bottom layer mean circulation extends from off the tip of Africa westward to the western boundary. In E11, the anticyclonic portion of this circulation pattern is similarly represented in the South Atlantic but extends a few hundred kilometers northeastward from Africa's tip into the Indian Ocean.

As the model retroflection is weaker in the new experiments, more of the Agulhas Current water leaks into the South Atlantic than in E11, and much of this additional leakage occurs in Agulhas rings. This is evident in the interface depth fluctuation (R.M.S.) fields of the new experiments by a tongue of large interface fluctuation extending from off Africa's tip west northwestward into the subtropical Atlantic for all except the lowest interface, of which the depth variation is suppressed by the relatively large g'. This tongue is pronounced for FCT1 and FCT2, but has less amplitude in FCT3 and especially in FCT4. The total and fluctuation kinetic energy in the retroflection region is also reduced from FCT2 to 4, suggesting again that as more upper ocean resolution is added, mechanisms for energy dissipation become more efficient.

One additional factor may account for some of the above-mentioned changes as upper ocean resolution is increased. As the horizontal mean thickness of the top layer is reduced, a larger fraction of it tends to concentrate toward the center of the subtropical gyres. The latitudes at which layers two and three outcrop along the subtropical convergence move northward, and the extent of layer 1 south of Africa becomes shorter. Layer 1 fluid leaks westward into the Atlantic in rings with relative ease since the retroflection is not strong, but the fluid attempting to return to the Indian Ocean after circulating through the South Atlantic has little room to do so south of the retroflection/ring formation area. The net result is that the mean layer 1 thickness becomes weighted toward the subtropical South Atlantic. In the 4-layer experiments FCT2 and FCT3, this weighting is compensated in layer 2, and in the 5-layer experiment FCT4 the compensation is in layers 2 and 3, such that the depths of the intermediate interfaces are not weighted especially toward either

the Atlantic or Indian Oceans. The differing mean stratifications to either side of the retroflection region, on the other hand, which result here from the specification of rather thin isopycnal layers at the top of the ocean in a purely wind-driven configuration, likely play a role in the dynamics of retroflection and ring formation of these experiments. This may result in the total absence of a mean retroflection in layer 1 in FCT3 and FCT4. BC showed that a strong temporal-mean layer thickness gradient between the southeast Atlantic and the southwest Indian Ocean, such that layer 1 thickness is greatest in the retroflection region, favors a strong retroflection. Such a gradient in layer 1 is inhibited from developing in FCT3 and FCT4 for the above-described reasons. We will return to this issue in the final section, where we propose an alternative approach.

4 THE MODEL AGULHAS RINGS

General characteristics of ring formation, size, and behavior among the experiments are given in Table 2. The maximum swirl velocity within the rings and the interface depth change from ring edge to center are good indications of how energetic the rings are. The translation speed is a combination of self-advection due to β and mean flow advection by the South Atlantic subtropical gyre once the rings are free of the African coast. In the remainder of this section, we discuss and illustrate the sensitivity of the model rings to upper ocean resolution and isopycnal outcropping.

Exp.	Diameter (km)	Interface Depth Change (db)	Maximum Swirl Velocity in a newly formed Ring ($m\ s^{-2}$)	Translation Speed west of Africa ($cm\ s^{-1}$)	Position of Separation from Agulhas	No. of Rings per 365 day Period
E11	280-300	300-350	1.25-1.5	6.2	Along southeast coast near Africa's tip	3
FCT1	200-240	300	0.75-1.0	7.5	South of Africa's tip.	4
FCT2		200-250	0.75	6.7	S to SW of Africa's tip.	5
FCT3			0.5-0.75		SW of Africa's tip.	
FCT4		150-200		6.5		

Table 2: Typical ring characteristics among the experiments. Blanks indicate no significant change from the previous experiment.

4.1 Three Layers (E11 and FCT1)

A typical event of ring formation in the quasi-isopycnic model simulation E11 has been examined in some detail by CB and is one of several rings described and compared with observation elsewhere in this volume (Chassignet *et al.*, 1989). The ring forms along the southeast coast of South Africa/Agulhas Bank near the tip. Its diameter shortly after cutoff from the main Agulhas is $\sim$ 300 km. The maximum swirl velocity is 1.2 m s^{-1} at a radius of

80 km. The interface 1 depth variation is ~300 db from ring edge to center. The ring first propogates westward at 4.3 cm s^{-1} as it rounds the tip of Africa, and then northwestward at 6.2 cm s^{-1} once it is absorbed into the South Atlantic subtropical circulation. Approximately 3 of these rings form per 365 day period in E11, and they account for essentially all of the leakage from the Indian into the South Atlantic Ocean.

In FCT1, the mean retroflecting Agulhas is not as strong and coherent as in E11 (Fig. 2). Another important difference is less of a tendency in FCT1 for the current core to separate from the coast upstream from the tip, carrying the isopycnal depth contours off with it. Ou and de Ruijter (1986) have shown that once an inertial current on a β-plane has separated from a coast with the orientation of the east side of the Agulhas Bank (toward the southwest), it has a tendency to make a counterclockwise turn. The mean Agulhas of E11 does this in a fairly abrupt fashion as it passes the tip of the Bank. In contrast, the layer 1 retroflection of FCT1 occurs over a broad region south of Africa's tip. In some sense, this is a more realistic configuration than in E11, as the real Agulhas Retroflection is generally located southwest of the tip of the Agulhas Bank, the region where ring formation is, therefore, most common (Lutjeharms, 1981; Lutjeharms and van Ballegooyen, 1984).

The rate at which top layer fluid leaks westward into the Atlantic is essentially the same in the two experiments. Another important difference, however, is in the layer 2 mean circulation patterns: that is, a small proportion of E11's total Sverdrup interior and retroflection are found in layer two, whereas they are approximately equally distributed between the top two layers in FCT1. In the latter as in the former, essentially all the leakage occurs within rings. In FCT1, both layers 1 and 2 exhibit $\sim 9 \times 10^6\, m^3\, s^{-1}$ leakage and in E11 the mean layer 2 leakage is $\sim 4 \times 10^6\, m^3\, s^{-1}$. It is apparent then that the transport and energetic expressions of the rings are more distributed over both layers 1 and 2 in FCT1 and are primarily in layer 1 for E11.

Typical instantaneous flow patterns a day or two preceding ring formation in the two experiments are illustrated in Fig. 3. Rings form and drift into the Atlantic at the rate of ~ 4 per 365 day period in FCT1. Since about the same mean rate of layer 1 leakage is accomplished in E11 and FCT1, the FCT1 rings must, therefore, have less volume and this is apparent in the Figure. The diameters of the two rings in E11 (Fig. 3a) are ~ 280-300 km and in FCT1 (Fig. 3b) ~ 200-220 km. The interface depth gradients around the rings are greater in FCT1, as might be expected due to the much reduced g', but the total change is ~ 300 m, as in E11. The strongest swirl velocities in the rings cutting off are 0.75 to 1.0 m s^{-1} and 1.25 to 1.5 m s^{-1} in FCT1 and E11, respectively, and similar relative values are seen in the rings propagating into the Atlantic. This is consistent with the above assertion that the retroflecting Agulhas, from which the rings are formed, is stronger and more coherent in E11. Because the FCT1 rings are smaller and less energetic, they become absorbed into the South Atlantic subtropical gyre and dissipate more quickly. The northwestward translation speed of FCT1 rings in the region west of the Bank is ~ 7.5 cm s^{-1}, compared

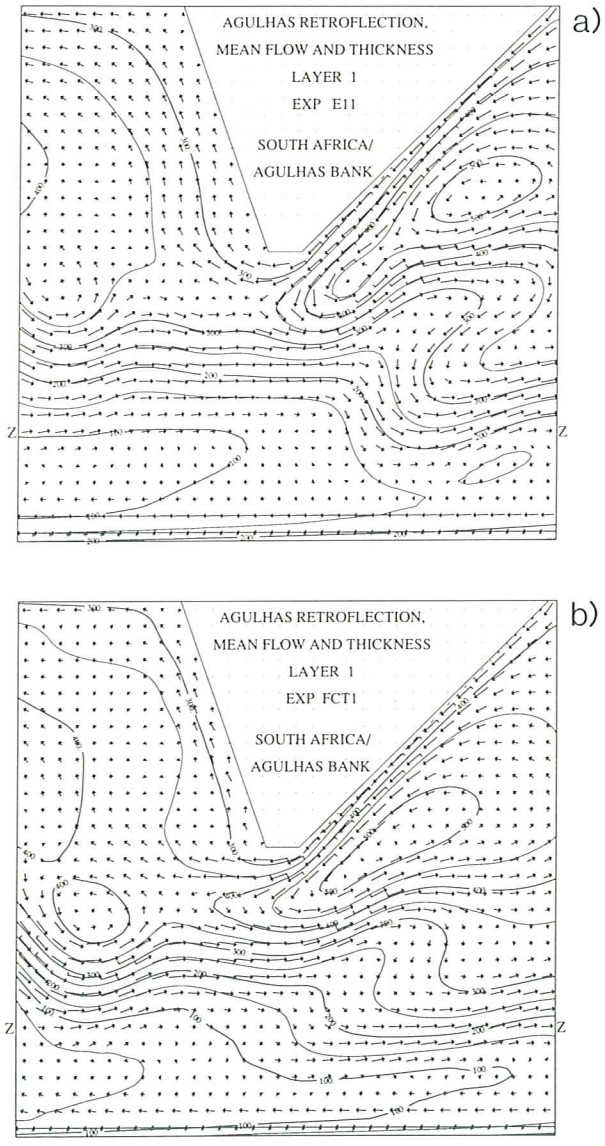

Figure 2: The layer 1 velocity and thickness fields averaged over the final 1825 days of the 3650 day experiments E11 (a) and FCT1 (b). Layer thickness is contoured in 50 db intervals. A full length arrow and each additional barb represents 0.25 m s^{-1} flow speed. Flow vectors are indicated for every other grid point. The latitude of wind curl zero is indicated by the Z's at the lower left and right.

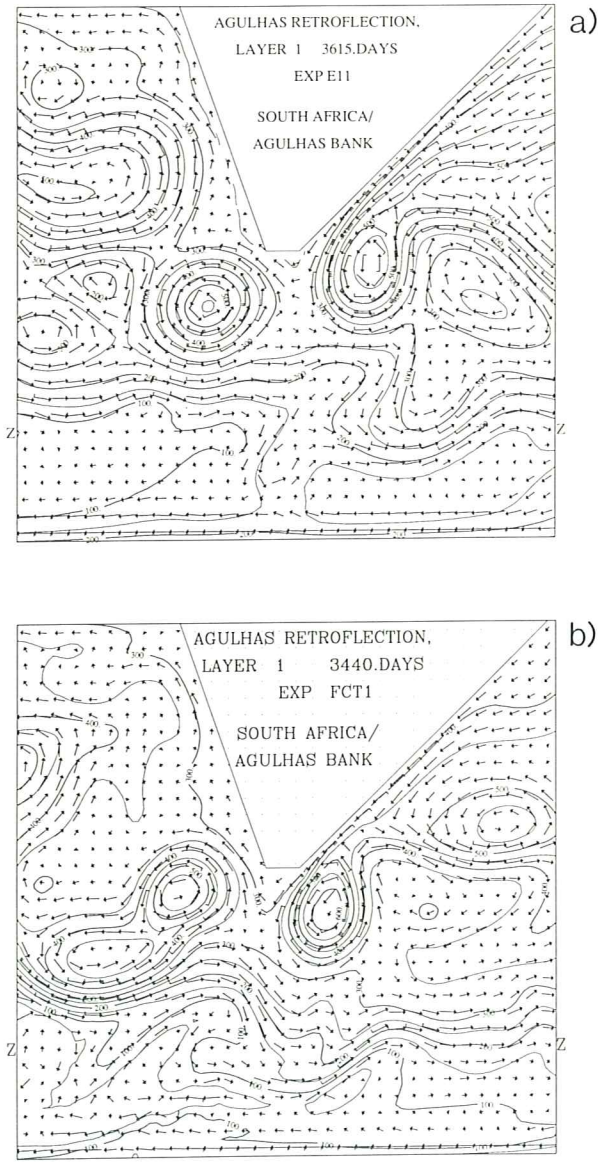

Figure 3: Typical layer 1 velocity and thickness fields as a ring is being formed in experiments E11 (a) and FCT1 (b). The contours and barbs are as in Fig. 2.

to the above-mentioned 6.2 cm s^{-1} for E11 rings, indicating a greater influence of the mean flow on the former.

As the upper ocean stratification is decreased and the intermediate stratification increased within a three-layer configuration, then, the Agulhas rings become smaller and weaker, but they form more often and in a more realistic position with respect to the tip of the model Agulhas Bank. They also have greater intermediate layer expression, as energy and momentum are transferred more easily from the top into the second layer. The latter is apparently also the reason for which the tendency for the interface between the upper layers to outcrop is suppressed, even though the density contrast between them has been greatly reduced. Interface 1 outcropping in FCT1 is sporadic and isolated, tending to occur mainly along the subtropical convergence[7] in the South Atlantic.

4.2 Four Layers (FCT2 and FCT3)

In this subsection, we further examine the model ring formation when upper ocean resolution is improved, first by dividing the upper 300 db into two layers of equal mean thickness and then by concentrating the coordinate layers more toward the upper surface. The net g' between the upper layers and the intermediate layer remains $\sim 0.01\ m\ s^{-1}$. In these cases, in contrast to FCT1, the first and second isopycnal layer interfaces typically outcrop along the subtropical convergence. In addition, the first interface outcrops around the eastern and northern edges of the subtropical gyres.

A snapshot of the layer 1 and 2 flow and interface 1 and 2 depth fields from FCT2 is depicted in Fig. 4. Three Agulhas rings are evident in the Figure. One is forming near the tip and two previously formed rings are propagating northwestward. Both of the interfaces are depressed in these rings, as we expect, but the depth gradient is weaker than for the rings of FCT1 (e.g., see Fig. 3b). Further, the total depth change from ring edge to center is 200 to 250 db, also smaller than in FCT1. This is typical of ring characteristics in FCT2-4 and confirms the conclusion of Section 3 that addition of upper ocean vertical resolution allows for more efficient dissipation of the energy input by the wind. In FCT2, the maximum swirl velocities within newly formed rings are typically 0.75 m s^{-1}. These rings are generally less energetic, then, than those of FCT1 although they have approximately the same mean diameters, 200-240 km. The mean translation rate is slower than in FCT1: 6.7 compared to 7.5 cm s^{-1}, likely because the mean flow is weaker, but also possibly because the ring's self-advection rate decreases as does its interface displacement (Nof, 1983). The rings typically separate from the Agulhas south of Africa's tip, so that the mean retroflection is broadly distributed there in the east-west direction, especially in layers 1 and 2. The intermediate layer 3 bears the strongest mean retroflection but also $\sim 9 \times 10^6\ m^3\ s^{-1}$ of leakage. Thus, as in FCT1, the transport and energetic expressions of the rings in this middle layer are very pronounced. From FCT1 to FCT2, the number of rings forming per 365 days increases

[7]The subtropical convergence in the real world divides the subtropical gyres from the northern edge of the Antarctic Circumpolar Current. In the model, we refer to the subtropical convergence as an ever-evolving line dividing the subpolar and subtropical gyres.

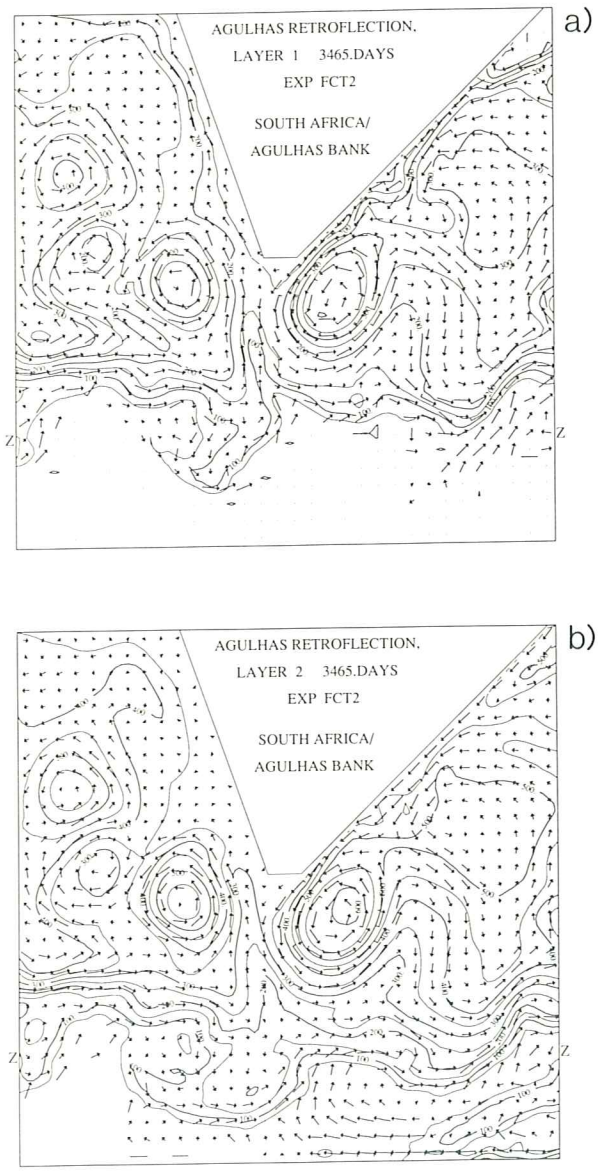

Figure 4: Typical layer 1 (a) and layer 2 (b) velocity and interface depth fields for experiment FCT2. The contours and barbs are as in Fig. 2. Grid points represented by dots indicate where the layer below is outcropped.

from 4 to 5, but the total volume of leakage remains about the same.

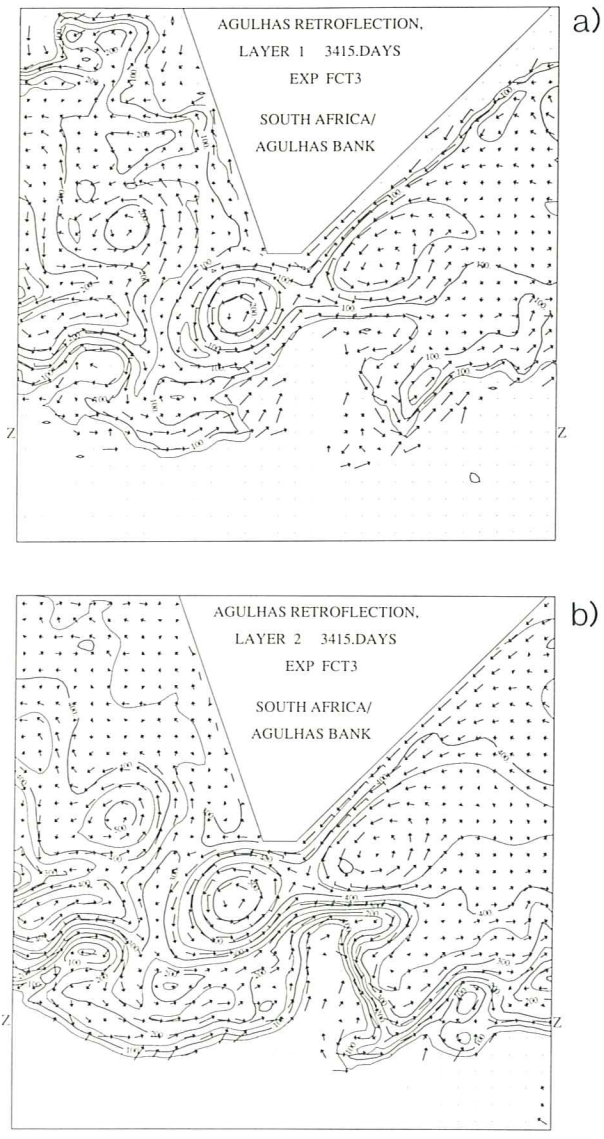

Figure 5: Instantaneous layer 1 (a) and layer 2 (b) velocity and interface depth fields for experiment FCT3 very close to an event of ring cutoff. The contours and barbs are as in Fig. 2 and the grid points represented by dots indicate where the layer below has outcropped.

Also evident in the Figure is a near-surface tongue of subpolar gyre fluid which is wedged between the developing and the previously formed ring just southwest of Africa's tip. It is quite common for the two water masses to interact in this fashion during ring formation

events in experiments FCT2-4 and in the real Agulhas Retroflection region (Lutjeharms, 1988, personal communication).

To encourage additional isopycnal outcropping, the mean thicknesses of the upper two layers are changed from 150 db each to 75 db and 175 db in the four-layer experiment FCT3. The data in Table 2 suggests that the impact which this has on the structure and behavior of the rings is a slight reduction in maximum swirl velocities to 0.5-0.75 m s^{-1}. Also, most of the rings are now west of Africa's tip before they cut off from the main Agulhas. From Table 1 we note that there is no mean retroflection in layer one, and the vertically integrated mass transport streamfunction (not shown) suggests that the mean retroflection intensity is slightly weaker than in FCT2. The individual layer streamfunctions (also not shown) suggest that there is no significant change in the rate of leakage from the Indian into the Atlantic. The rings and the mean circulation, then, South of Africa's tip are less energetic as resolution is concentrated toward the upper surface, suggesting again that the energy input by the wind is dissipated more effectively.

An illustration exhibiting the FCT3 preference for a more westerly ring formation position is given in Fig. 5, where instantaneous mass and flow fields for layers 1 and 2 are depicted just prior to ring cutoff. Note that a portion of the Agulhas turns back toward the Indian Ocean near the southeast tip of the shelf break geometry, but another significant portion continues around the outer edge of the developing ring circulation. Between the two is an intrusion of subpolar gyre fluid as much as 240 km north of the wind curl zero latitude. This intrusion, strongly evidenced in the 2nd interface depth (Fig. 5b) contours, is associated with and is likely playing an important role in the ring formation event. The subtropical front is sharply inclined in general, but especially here where the depth of the 2nd interface increases from less than 50 db to 400 db over a distance of $\sim$ 60 km.

4.3 Five Layers (FCT4)

The rings of FCT4, in which two upper layers now have mean thicknesses of 75 db, the third 100 db, the intermediate layer 950 db, and the bottom layer 3800 db (as in all experiments), are even less energetic than in FCT3. Horizontal plots of total and eddy kinetic energy (not shown) reveal that the retroflection region is 20-30% less energetic than in FCT3. From column 3 of Table 2 we note that the interface depth change from the ring edge to center is typically only 150 to 200 m, and this is true for all three of the upper ocean interfaces. The maximum swirl velocities are generally little more than 0.5 m s^{-1}. Again, this further increase in upper ocean resolution has enhanced the transfer of energy input by the wind to the intermediate layer, as well as allowed for more efficient dissipation through release of instabilities. Also, as pointed out at the end of Section 3, the energetic and dynamical character of the retroflection region may be significantly influenced in FCT3-4 by the fact that layer 1 fluid tends to accumulate in the South Atlantic subtropical gyre, finding it somewhat difficult to return to the Indian Ocean in the short distance south of Africa to its outcrop. This configuration is an artifact of the lack of thermohaline forcing

in the model. In actuality, some of the warm fluid leaking from the Indian into the Atlantic returns to the Indian Ocean as modified denser water after circulating through the South Atlantic. An accounting for such conversion must be made to determine the effect of the non-thermohaline forced circumstances on the retroflection dynamics. We will return to this issue in the closing remarks.

Of particular significance in the experiments with more upper ocean resolution is the realistic tendency for rings to cut away from the Agulhas farther south and west than in E11 and FCT1. This is perhaps the factor most responsible for increased interaction with the fluid from the subtropical/polar front in FCT2-4. Such volatile interaction in FCT4 is illustrated in Fig. 6, where layer 3 flow and interface 3 depth are depicted at two instants 25 days apart. As in Fig. 5, a pronounced intrusion of subpolar fluid is involved in the ring formation event near Day 3440 (Fig. 6a). In the subsequent snapshot (Fig. 6b), this intrusion has shifted eastward where it is influencing the formation of the next ring. This interaction in the model is especially significant because satellite imagery commonly displays filaments of cold surface water from the northern edge of the ACC between the Retroflection and a newly formed ring (Lutjeharms, 1988, personal communication).

5 SUMMARY AND DISCUSSION

The sensitivity of Agulhas retroflection and ring formation in an idealized model of the South Atlantic-Indian Ocean to increases in upper ocean vertical resolution and isopycnal outcropping has been explored. Here we have described a first series of experiments with a pure-isopycnic coordinate model which handles the outcropping of coordinate surfaces in a robust fashion, replacing the quasi-isopycnic coordinate model used in previously reported work. To encourage isopycnal outcropping, first, the relative strengths of the interface density jumps in the 3-layer framework are reversed. The uppermost interface g' is reduced from 0.02 to 0.01 m s^{-2}, but a major impact is the more rapid transfer of energy from layer 1 to 2, as well as more efficient dissipation of energy input by the wind. Thus, isopycnal outcropping is not a predominant feature of the experiment. The retroflection is slightly weakened and the rings formed are smaller and less energetic than in the case with the stronger upper interface g', but they have more intermediate layer expression.

When the number of layers is increased first to 4 and then 5, the strength of the retroflection and the energetic magnitudes of the retroflection activity continues to decrease. The rings tend to separate from the main Agulhas more often and at a more southwesterly position, however, which is a trend more toward the position where real Agulhas rings form with respect to the Agulhas Bank. Likely because of this more southerly location, intrusions of subpolar origin fluid are quite often found playing an active role in the ring formation events, as is known to happen in the Retroflection area.

A preliminary conclusion from these results is that reduced static stability and improved vertical resolution near the model ocean surface both lead to more efficient dissipation of

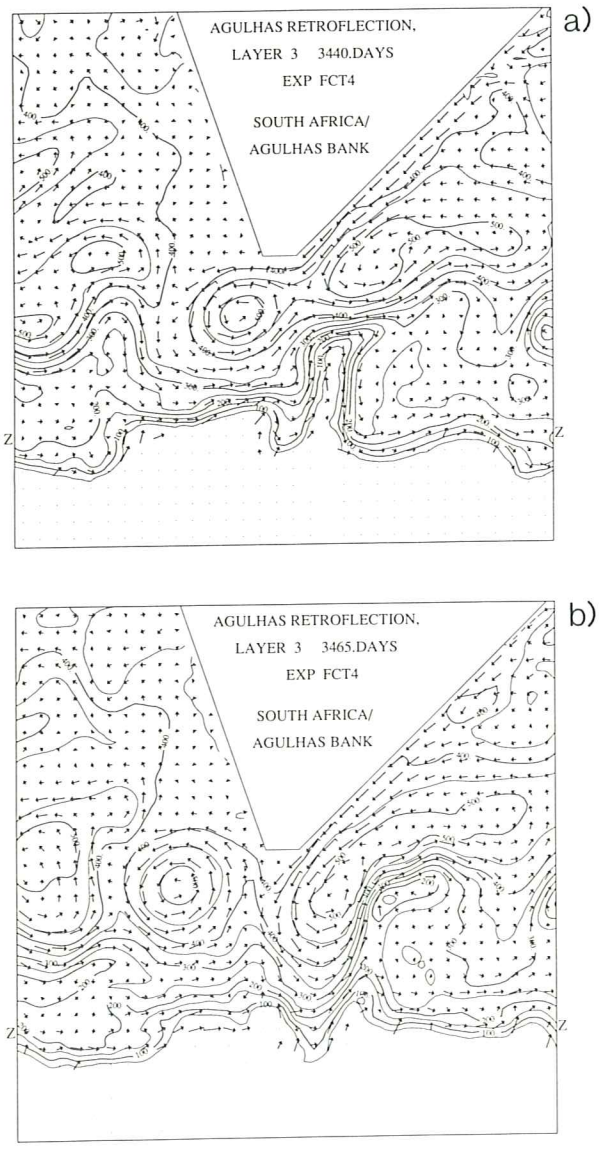

Figure 6: Instantaneous layer 3 flow patterns and interface 3 depth fields 25 days apart in FCT4. Note the intrusion of subpolar fluid associated with development of two rings. The contours and barbs are as in Fig. 2 and the grid points represented by dots indicate where the layer below has outcropped.

the energy input by the wind at the surface. In the first case, the upper ocean flows become unstable more rapidly, and in the second, the release of instability is apparently better resolved. A thorough energetics analysis of the experiments would be required to verify the second assertion. Chassignet and Boudra (1988) found coherent peaks in basin-averaged barotropic and baroclinic eneergy conversion to coincide with events of Agulhas ring cutoff in the quasi-isopycnic experiment E11, and they concluded that a weak mixed barotropic/baroclinic instability is associated with ring formation in the experiment. Due to the relative weakness of the rings generated in the experiments FCT2 to FCT4 here, it seems that peaks in the basin-averaged energetics would be less prominent and that dynamical instabilities play a less significant role in the formation process. What is mainly apparent here is that the onset of instabilities occurs at a lower level of basin available potential energy, preventing the circulation from reaching the mean energetic intensity of E11.

In order to verify or refute the above preliminary conclusion, additional experimentation is also suggested. In particular, a series of pure-isopycnic coordinate experiments in which the mean upper ocean static stability is similar to that in E11, and the resolution is increased as in the series here FCT1-FCT4, would be helpful. Secondly, some representation of thermohaline forcing must be incorporated into the experiments with very thin upper layers. Without this, layer 1 fluid tends to become trapped in the South Atlantic subtropical gyre. In the real South Atlantic/Indian ocean, pools of lightest fluid are generally isolated from each other in the southwest portions of the basins. Small parcels of the Indian pool occasionally break away into the southeast Atlantic through the retroflection region. Such light fluid is then modified on its journey which will eventually carry it across the equator or around the South Atlantic subtropical gyre and back into the Indian Ocean south of Africa. In the latter case, the fluid is denser than when it originally drifted into the Atlantic. Models of the type discussed here must ultimately incorporate buoyancy gain/loss. In the near future, we propose to develop the capability in the model to convert layer 1 fluid in the South Atlantic to intermediate layer fluid, so that it may freely return to the Indian Ocean south of Africa, where it will return to the upper layer near the eastern boundary. The conversion rate may be varied to determine the impact of thermohaline circulation strength on the retroflection dynamics.

Finally, once more computer power becomes available, the sensitivity of the results to increased horizontal resolution should be tested. As more vertical resolution is introduced, the radii of deformation associated with the new vertical modes become progressively smaller. In order to resolve the baroclinic processes associated with these modes, finer horizontal grid spacing should be used. At the current stage of computer technology, such sensitivity studies with 5 or 10 km grid spacing are feasible only with filtered models[8] which allow use of a much larger time step than primitive equations models.

[8]Such as those based on the balance equation and the quasi-geostrophic approximation.

6 ACKNOWLEDGEMENTS

This work has been supported by the Office of Naval Research Grant No. N00014-87-G0116. The calculations have been performed on the Cray computers at the Naval Research Laboratory and at the National Center for Atmospheric Research (NCAR). NCAR is sponsored by the National Science Foundation.

7 REFERENCES

Bleck, R. and Boudra, D.B., 1981. Initial testing of a numerical ocean circulation model using a hybrid (quasi-isopycnic) vertical coordinate. J. Phys. Oceanogr., 11: 755-770.

Bleck, R. and Boudra, D.B., 1986. Wind-driven spin-up in eddy-resolving ocean models formulated in isobaric and isopycnic coordinates. J. Geophys. Res., 91(C6): 7611-7621.

Boris, J.P. and D.L. Book, 1973. Flux-corrected transport, I, SHASTA, a fluid transport algorithm that works. J. Computat. Phys., 11: 38-69.

Boudra, D.B. and De Ruijter, W.P.M., 1986. The wind-driven circulation of the South Atlantic-Indian Ocean. II: Experiments using a multi-layer numerical model. Deep-Sea Res., 33: 447-482.

Boudra, D.B. and Chassignet, E.P., 1988. Dynamics of Agulhas Retroflection and ring formation in a numerical model. I: The vorticity balance. J. Phys. Oceanogr., 18: 280-303.

Charney, J.G., 1955. The Gulf Stream as an inertial boundary layer. Proc. Natl. Acad. Sci. U.S.A., 41: 731-740.

Chassignet, E.P. and Boudra, D.B., 1988. Dynamics of Agulhas Retroflection and ring formation in a numerical model. II: Energetics and ring formation. J. Phys. Oceanogr., 18: 304-319.

Chassignet, E.P., Olson, D.B., and Boudra, D.B., 1989. Evolution of rings in numerical models and observations. In *Mesoscale Synoptic Coherent Structures in Geophysical Turbulence*. J.C.J. Nihoul and B.M. Jamart, Eds. Elsevier, Amsterdam. Submitted.

De Ruijter, W., 1982. Asymptotic analysis of the Agulhas and Brazil Current system. J. Phys. Oceanogr., 12: 361-373.

De Ruijter, W.P.M. and Boudra, D.B., 1985. The wind-driven circulation of the South Atlantic-Indian Ocean. I: Experiments in a one-layer model. Deep-Sea Res., 32: 557-574.

Gordon, A.L., 1985. Indian-Atlantic transfer of thermocline water at the Agulhas Retroflection. Science, 227: 1030-1033.

Gordon, A.L., 1986. Interocean exchange of thermocline water. J. Geophys. Res., 73: 531-534.

Hellerman, S. and Rosenstein, M., 1983. Normal monthly wind stress over the world ocean with error estimates. J. Phys. Oceanogr., 13: 1093-1104.

Lutjeharms, J.R.E., 1981. Spatial scales and intensities of circulation of the ocean areas adjacent to South Africa. Deep-Sea Res., 28A: 1289-1302.

Lutjeharms, J.R.E. and van Ballegooyen, R.C., 1984. Topographic control in the Agulhas Current System. Deep-Sea Res., 31: 1321-1337.

Lutjeharms, J.R.E. and Gordon, A.L., 1987. Shedding of an Agulhas ring observed at sea. Nature, 325: 138-140.

Moore, D.W. and Niiler, P.P., 1974. A two-layer model for the separation of inertial boundary currents. J. Mar. Res., 32: 457-484.

Nof, D., 1983. On the migration of isolated eddies with application to Gulf Stream rings. J. Mar. Res., 41: 399-425.

Olson, D.B. and Evans, R.H., 1986. Rings of the Agulhas. Deep-Sea Res., 33: 27-42.

Ou, H.W. and De Ruijter, W.P.M., 1986: Separation of an inertial boundary current from a curved coastline. 16: 280-289.

Parsons, A.T., 1969. A two-layer model of Gulf Stream separation. J. Fluid Mech., 39: 511-528.

Veronis, G., 1973. Model of world ocean circulation: I. Wind-driven, two layer. J. Mar. Res., 31: 228-288.

Zalesak, S.T., 1979: Fully multi-dimensional flux-corrected transport algorithm for fluids. J. Computat. Phys., 31: 335-362.